(Received 13 July 2024, Accepted 12 August 2024, Scheduled 25 August 2024)

Negative Group Delay Prototype Filter Based on the Ratio of Two Classical Chebyshev Filter Transfer Functions

Miodrag Kandic[1, 2, *] and Greg E. Bridges[1, 3]

[1] *Department of Electrical and Computer Engineering, University of Manitoba, Winnipeg, Manitoba, Canada*
[2] *ORCID: 0000-0002-3673-4706*
[3] *ORCID: 0000-0001-8147-9882*

ABSTRACT: A Negative Group Delay (NGD) prototype filter design, based on the ratio of two Chebyshev filter transfer functions, is presented. The two transfer functions are of the same order, but with different in-band ripple amplitudes and different 3 dB-bandwidths. The overall transfer function exhibits both an in-band ripple and an out-of-band steep-slope magnitude transition characteristic of a Chebyshev filter, while also exhibiting an in-band NGD. For high-order designs and in the upper asymptotic limit, the NGD-bandwidth product of the filter is shown to be a linear function of out-of-band gain in decibels. A resonator-based methodology is used to show how frequency upshifted filter designs can be implemented in a Sallen-Key topology or in an all-passive ladder topology. An in-band combined magnitude/phase distortion metric is evaluated for examples of the NGD filter. It is shown that the distortion metric is proportional to the design order, the in-band ripple amplitude, and the out-of-band gain. For a prescribed distortion metric value, it is demonstrated that the proposed design can achieve a higher NGD-bandwidth product than an equivalent Butterworth design, which has a flat in-band magnitude characteristic. Additionally, input waveforms with bandwidths extending to the entire frequency range where the group delay is negative (typically larger than the 3 dB-bandwidth) should not be applied to this filter design as it results in strong levels of distortion.

1. INTRODUCTION

Negative group delay (NGD) phenomenon is observed in anomalous dispersion media, within finite frequency bands. Since group delay is defined as a negative derivative of the phase characteristic in the frequency domain, NGD is manifested via positive phase characteristic slope. In the time domain, NGD is manifested via reshaping of an analytical waveform, where certain waveform features (such as pulse peak) are formed at the medium output before they are observed at the input. Causality is not violated in this case, since any non-analytical part of the waveform (such as onset, or "front") was shown not to exceed the luminal velocity [1–3]. In addition to NGD, negative refractive index [4], superluminal [5], simultaneous negative phase and group velocity [6], are some of other abnormal wave propagation examples.

Based on magnitude and phase characteristic dependency described by Kramers-Kronig relations in causal media, it is shown that the magnitude response has a minimum within a frequency band exhibiting NGD phenomenon [7]. For gain-uncompensated designs, this translates into maximum Signal Attenuation (SA) being observed within the NGD bandwidth. For gain-compensated designs SA is corrected at the expense of introducing an out-of-band gain. Regardless of the gain compensation being applied or not, a relative out-of-band gain compared to in-band is present in all NGD designs. It is shown that the out-of-band gain is proportional to undesired amplification of transients in the output waveform, when pulses with non-analytical discontinuities, such as defined "turn on/off" points in time, are propagated [8–11]. Further, any type of discontinuity in the waveform or its derivatives was demonstrated to cause a transient response associated with an out-of-band gain [12].

A trade-off relationship exists between the desired NGD-bandwidth product and the undesired maximum out-of-band gain, and it was functionally quantified for studied media in [8–10]. The NGD-bandwidth product was shown to have a square root relationship with the out-of-band gain given in decibels, in the upper asymptotic limit for a distributed medium composed of a large number of cascaded identical 1st-order NGD circuits at baseband frequencies [8]. Equivalently, the same square root relationship applies to cascaded identical 2nd-order NGD circuits tuned at a non-zero center frequency. Similarly, a causal medium was engineered from a chosen in-band positive slope linear phase characteristic (flat in-band NGD characteristic), with Kramers-Kronig relations employed to obtain the magnitude characteristic resulting in another square root relationship [9], just with a higher scaling factor than [8]. The NGD-bandwidth product was shown to have a power of 3/4 relationship with the out-of-band gain given in decibels, in the upper asymptotic limit for a distributed medium comprised of a large number of cascaded identical 2nd-order NGD circuits at baseband frequencies [10].

An NGD filter based on an Nth-order capped reciprocal-Butterworth low-pass transfer function is presented in [13]. For

* Corresponding author: Miodrag Kandic (Miodrag.Kandic@umanitoba.ca/ kandic@ngdfilters.com).

cascaded identical Nth-order capped reciprocal-Butterworth circuits at baseband frequencies, the NGD-bandwidth product was shown to be proportional to the out-of-band gain given in decibels raised to the power of $(1 - 1/2N)$ [13], which is a generalization of the trend observed for $N = 1$ in [8] and for $N = 2$ in [10]. Further, the capped reciprocal-Butterworth design achieves an NGD-bandwidth product that in the upper asymptotic limit as the design order approaches infinity is a linear function of out-of-band gain in decibels [13].

In this paper, the conceptual NGD transfer function synthesis presented in [13] is applied to the reciprocal of the Chebyshev low-pass transfer function, with its out-of-band gain capped at a finite constant value by a multiplying low-pass Chebyshev filter transfer function with the same order and a smaller in-band ripple. The overall design is feasible due to having a finite out-of-band gain. Such synthesized capped reciprocal-Chebyshev transfer function is shown to exhibit a higher NGD-bandwidth product than the capped reciprocal-Butterworth function presented in [13], for the same design order and out-of-band gain. It is shown that resonator-based design implementations in a Sallen-Key topology, as well as in an all-passive ladder topology are feasible for the prototype NGD transfer function translated to a higher center frequency. The prototype capped reciprocal-Chebyshev design achieves an NGD-bandwidth product that in the upper asymptotic limit for high design order values is the same linear function of out-of-band gain in decibels associated with capped reciprocal-Butterworth design in [13], but further improved by an offset which is a linear function of the design order. Parameters of this offset function are shown to be proportional to the in-band ripple value.

For selected input time-domain waveforms applied to the proposed design, an in-band combined magnitude/phase distortion metric reported in [14, 15] and slightly modified as in [10, 13] is evaluated. When the bandwidth used for waveform propagation is kept at 3 dB, to have the distortion metric below a prescribed acceptable value it is shown that the design order, and/or the in-band ripple, and/or the out-of-band gain of the proposed capped reciprocal-Chebyshev design need to be kept below certain values. Common performance parameters that NGD designs are compared for, such as designs in [8, 16–32], are the achieved NGD-bandwidth product and the trade-off quantity out-of-band gain (which for gain-uncompensated designs translates into signal attenuation). In addition, it would be beneficial to check any NGD design for in-band magnitude/phase distortion as discussed in [10, 13] and is checked in this paper. Further, many NGD designs in the literature report the entire bandwidth where the group delay is negative, $\tau(\omega) < 0$ (typically larger than 3 dB-bandwidth). The usefulness of such bandwidth should be qualified for any NGD design since it may result in strong levels of distortion of propagated waveforms, as pointed in [13, 33]. In this paper, it was demonstrated that for the studied capped reciprocal-Chebyshev designs, the use of 3 dB-bandwidth is also preferred over the $\tau(\omega) < 0$ bandwidth, to keep distortion at an acceptable level.

2. PROTOTYPE NGD FILTER BASED ON CAPPED RECIPROCAL LOW-PASS CHEBYSHEV FILTER TRANSFER FUNCTION

Baseband NGD transfer functions based on 1st and 2nd-order rational transfer functions are discussed in [9, 10, 34, 35], while designs involving non-integer power functions were presented in [36]. NGD-exhibiting transfer function based on a ratio of two Nth-order low-pass Butterworth filter transfer functions with different bandwidths is reported in [13]. It was shown that this baseband transfer function can be factorized into a product of non-identical 2nd-order rational transfer function(s), and for odd-order designs a 1st-order rational transfer function is included in the product as well. The same factorization properties are applicable to the design presented in this paper.

As a variation of the concept presented in [13], a transfer function based on a ratio of two Nth-order low-pass Chebyshev filter transfer functions with different in-band ripples (and therefore different 3 dB-bandwidths as well), is given by:

$$H(j\omega) = H_{reciprocal\text{-}LP}(j\omega) \cdot H_{capping\text{-}LP}(j\omega)$$

$$= \frac{1}{H_{LP\text{-}ripple\text{-}\varepsilon}(j\omega)} \cdot H_{LP\text{-}ripple\text{-}\varepsilon/A}(j\omega). \quad (1)$$

It can be shown that NGD exists around the center frequency, if the in-band ripple of the capping function, ε/A, is smaller than that of the reciprocal function, ε (i.e., out-of-band gain $A > 1$). A patent application details the design process [37]. Fig. 1 illustrates a magnitude plot of a capped reciprocal-Chebyshev design transfer function (1), showing a finite out-of-band gain, A. The shown example can also be scaled to represent a gain-uncompensated design, without affecting the group delay characteristic.

From Fig. 1 it is evident that the overall proposed capped reciprocal-Chebyshev design satisfies the requirement from [7], that for an NGD design transfer function magnitude minimum occurs within the in-band around the center frequency. The proposed design core term producing the NGD in (1) is a reciprocal function of a Chebyshev low-pass filter transfer function, $1/H_{LP\text{-}ripple\text{-}\varepsilon}(j\omega)$, with a ripple amplitude ε (between 0

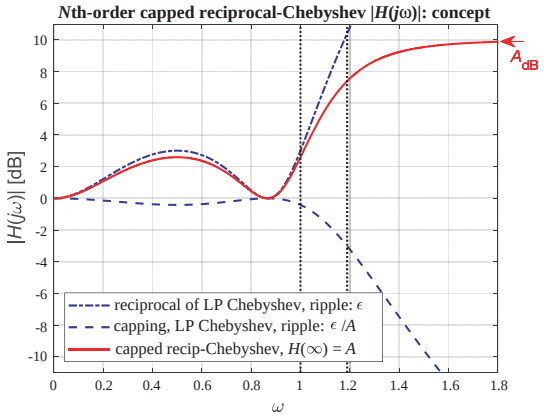

FIGURE 1. Example 3rd-order capped reciprocal-Chebyshev NGD baseband design, $A = 3.162$ ($A_{\text{dB}} = 10$ dB), ripple $\varepsilon = 1$ (3 dB), capping ripple $\varepsilon/A = 0.316$ (0.414 dB).

and 1, where 1 corresponds to 3 dB) exhibited within the 3 dB-bandwidth. An infinite out-of-band gain is associated with the reciprocal function term alone, or an infinite center frequency attenuation in its gain-uncompensated version. Therefore, an out-of-band gain "capping" is needed to make the design feasible. Multiplying the reciprocal transfer function with a low-pass Chebyshev transfer function, $H_{LP\text{-}ripple\text{-}\varepsilon/A}(j\omega)$, as given in (1), achieves the needed out-of-band capping. Further, it turns out that the in-band ripple of the capping function needs to be ε/A, in order to yield an out-of-band gain A of the overall transfer function.

The in-band part of the reciprocal function is not significantly affected due to the smaller in-band ripple of the capping function, which is especially the case for designs with larger out-of-band gain values A. Further, positive out-of-band magnitude response slope of the reciprocal function is almost perfectly canceled by the capping function past its 3 dB cut-off frequency, since both functions are of the same order and the same Chebyshev type. Since the capping function in (1) corresponds to the classical low-pass Chebyshev filter, it emerges as the denominator polynomial of the overall transfer function. Therefore, the overall transfer function in (1) is inherently stable since it has poles in the $s = j\omega$ complex Left Half-Plane (LHP). The proposed capped reciprocal-Chebyshev design baseband transfer function of an odd Nth-order is given by:

$$H_{N\text{-}odd}(j\omega) = A\frac{\omega' - j\cdot k_1}{\omega' - j\cdot k_2}\prod_{m=1}^{(N-1)/2}\left(\frac{\omega'^2 - j\cdot 2k_1\cdot\sin\left(\frac{2m-1}{2N}\pi\right)\omega' - \left(k_1^2+\cos^2\left(\frac{2m-1}{N}\frac{\pi}{2}\right)\right)}{\omega'^2 - j\cdot 2k_1'\cdot\sin\left(\frac{2m-1}{2N}\pi\right)\omega' - \left(k_1'^2+\cos^2\left(\frac{2m-1}{N}\frac{\pi}{2}\right)\right)}\right), \quad (2a)$$

where the factorized functions' parameters are as in Nth-order Chebyshev low-pass filter (chosen in-band ripple given in decibels is R_{dB}, with values between 0 dB and 3 dB):

$$\varepsilon = \sqrt{10^{(R_{\text{dB}}/10)}-1}, \quad (2b)$$

$$k_1 = \sinh\left(\frac{1}{N}\cdot\sinh^{-1}\left(\frac{1}{\varepsilon}\right)\right),$$

$$k_1' = \sinh\left(\frac{1}{N}\cdot\sinh^{-1}\left(\frac{A}{\varepsilon}\right)\right), \quad (2c)$$

and the normalized frequency ω' represents frequency ω scaled by a 3 dB cut-off frequency correction factor, given by:

$$\omega' = \frac{\omega}{C_{\omega-3\,\text{dB}}},$$

$$C_{\omega-3\,\text{dB}} = \cosh\left(\frac{1}{N}\cdot\cosh^{-1}\left(\frac{1}{\varepsilon\sqrt{1-2/A^2}}\right)\right). \quad (2d)$$

Even-order design transfer function is similar to expression (2a), just with the first order rational term dropped and the product upper limit changed to $N/2$. However, as it will be discussed later, even-order capped reciprocal-Chebyshev designs have a reduced center frequency NGD compared to capped reciprocal-Butterworth design presented in [13], as a contrast to odd-order designs which increase it. Therefore, this paper is focused on odd-order capped reciprocal-Chebyshev designs.

As a correction factor numerical example given by (2d), for in-band ripple $R_{\text{dB}} = 3\,\text{dB}$ ($\varepsilon = 1$) and out-of-band gain $A = 10$ (20 dB), the 3 dB cut-off frequency correction factor for order $N = 3$ yields $C_{\omega-3\,\text{dB}} = 0.9989$. For higher orders or higher out-of-band gain values, the resulting value is even closer to 1.0, which renders the correction factor negligible in those cases. A lower ripple of R_{dB} =0.5 dB for example, for out-of-band gain $A = 100$ (40 dB) yields $C_{\omega-3\,\text{dB}} = 0.8565$, 0.9440, for $N = 3, 5$, respectively. The correction factor for lower ripple values is sensitive to the order of the design, but not as sensitive to the out-of-band gain values (the previous example values would only slightly decrease to 0.8550 and 0.9434, respectively, when out-of-band gain is reduced from 40 dB to 20 dB).

From expressions (2a)–(2d), example transfer functions for several designs with different orders and in-band ripple values, and for given out-of-band gain $A = 100$ (40 dB), are given by:

$$H_{3rd-0.5\,\text{dB}}(j\omega) = 100\left(\frac{\omega - j\cdot 0.5366}{\omega - j\cdot 3.5046}\right)\cdot\left(\frac{\omega^2 - j\cdot 0.5366\omega - 0.9155^2}{\omega^2 - j\cdot 3.5046\omega - 3.5822^2}\right), \quad (3a)$$

$$H_{3rd-3\,\text{dB}}(j\omega) = 100\left(\frac{\omega - j\cdot 0.2980}{\omega - j\cdot 2.8385}\right)\cdot\left(\frac{\omega^2 - j\cdot 0.2980\omega - 0.9159^2}{\omega^2 - j\cdot 2.8385\omega - 2.9677^2}\right), \quad (3b)$$

$$H_{5th-0.5\,\text{dB}}(j\omega) = 100\left(\frac{\omega - j\cdot 0.3420}{\omega - j\cdot 1.5483}\right)\cdot\left(\frac{\omega^2 - j\cdot 0.2114\omega - 0.9608^2}{\omega^2 - j\cdot 0.9569\omega - 1.7898^2}\right)\cdot\left(\frac{\omega^2 - j\cdot 0.5534\omega - 0.6519^2}{\omega^2 - j\cdot 2.5052\omega - 1.6447^2}\right). \quad (3c)$$

Expression (2a) and correspondingly (3a)–(3c) represent gain-compensated designs. Dividing these expressions by the out-of-band gain A results in the center frequency magnitude attenuation $1/A$ ($-A_{\text{dB}}$) and the out-of-band magnitude characteristic below 1 (0 dB). This scaling does not affect the group delay response. Resulting gain-uncompensated magnitude plots for several different design orders are shown in Fig. 2(a), for several different center frequency attenuations (relative out-of-band gains) in Fig. 3(a), and in Fig. (4a) for several different in-band ripple amplitudes, while the other two parameters are kept constant in each case. Corresponding group delay plots

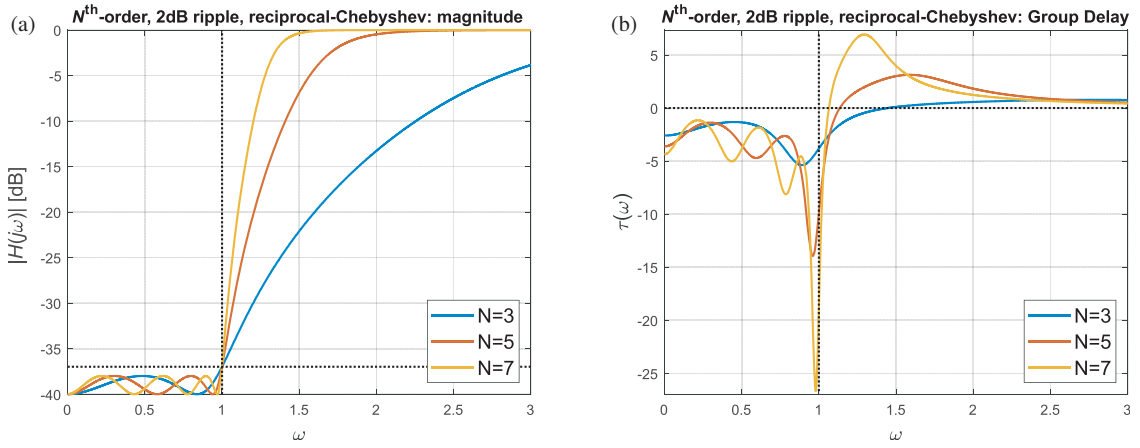

FIGURE 2. Proposed capped reciprocal-Chebyshev baseband transfer function NGD design with out-of-band gain $A = 100$ (40 dB), in-band ripple of $R_{\text{dB}} = 2$ dB and $N = 3, 5, 7$ order, (a) magnitude and (b) group delay plot.

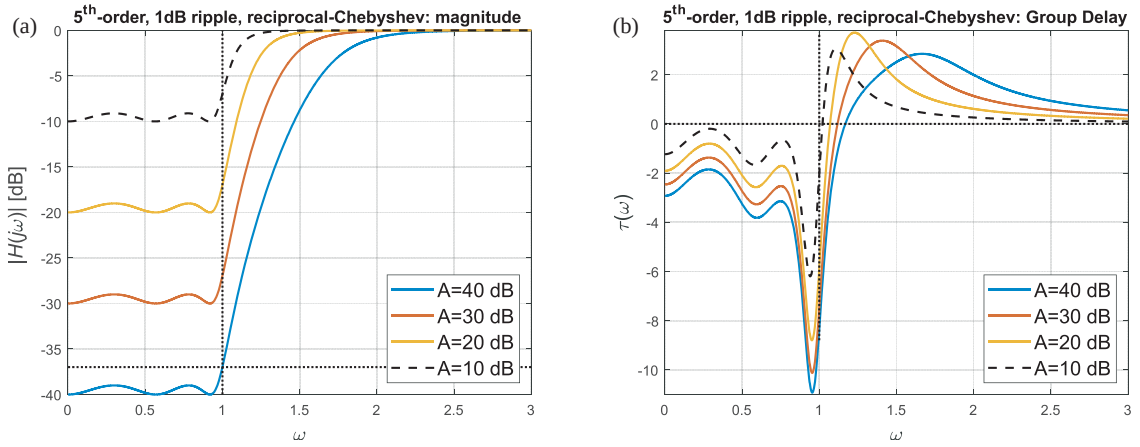

FIGURE 3. Capped reciprocal-Chebyshev baseband 5th-order design with in-band ripple of $R_{\text{dB}} = 1$ dB and with out-of-band gains $A = 10$ dB, 20 dB, 30 dB, 40 dB, (a) magnitude and (b) group delay plots.

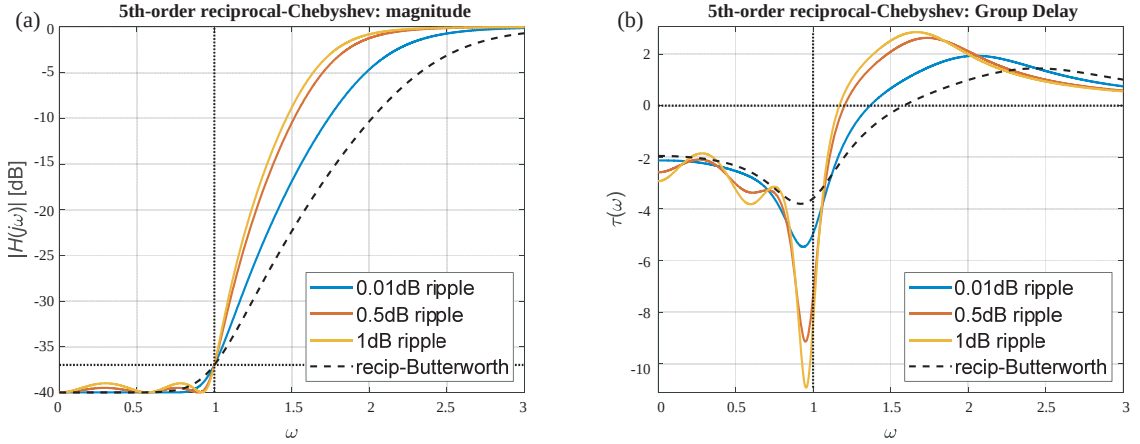

FIGURE 4. Capped reciprocal-Chebyshev baseband 5th-order design with out-of-band gain $A = 100$ (40 dB), and with in-band ripples of $R_{\text{dB}} = 0.01$ dB, 0.5 dB, 1 dB, (a) magnitude and (b) group delay plots.

are shown in Figs. 2(b), 3(b), and 4(b), respectively. Fig. (2a) demonstrates that increasing the order of the proposed design, while keeping the in-band ripple amplitude and out-of-band gain constant results in a steeper magnitude characteristic transition from in-band to out-of-band region. Further, Fig. (2b) demonstrates that the described order increase also results in the center frequency NGD increase, as well as an increase in the overall group delay variation (a trade-off, resulting in increased waveform distortion). Fig. (3b) demonstrates that increasing the out-of-band gain of the proposed design, while keeping the

in-band ripple amplitude and the design order constant, results in a seemingly linear (with out-of-band gain in dB) increase of the center frequency NGD. This seemingly linear relationship is further analyzed later in this paper.

The effect of in-band ripple amplitude variation on the magnitude and group delay characteristics is captured in Figs. 4(a) and 4(b), respectively. An almost negligible in-band ripple example of 0.01 dB is chosen to demonstrate its close in-band magnitude characteristic match to capped reciprocal-Butterworth design [13], with the in-band to out-of-band magnitude characteristic transition significantly steeper however, even for such small ripple design. Similarly, Fig. (4b) demonstrates a close in-band group delay characteristic match to capped reciprocal-Butterworth design, for the same small in-band ripple example of 0.01 dB. Increased in-band ripple results in progressively steeper out-of-band magnitude transitions, as well as in the center frequency NGD further increased relative to the corresponding capped reciprocal-Butterworth example.

Therefore, the proposed NGD capped reciprocal-Chebyshev design can be interpreted as a design that exhibits a group delay characteristic that "builds" on the capped reciprocal-Butterworth design reported in [13]. A negligible in-band ripple in the capped reciprocal-Chebyshev design corresponds to the capped reciprocal-Butterworth design, and a further ripple amplitude increase results in an increase of the center frequency NGD as shown in Fig. 4(b) for odd-order designs, due to the concave ripple shape. Conversely, even-order designs have a convex ripple shape, which effectively reduces the center frequency NGD compared to the capped reciprocal-Butterworth design, which is the reason that this paper focuses on odd-order capped reciprocal-Chebyshev designs. The trade-off associated with the proposed design is an in-band distortion increase in the magnitude and group delay characteristics, as will be discussed later in the paper.

The 1st-order factorized rational function general form present in the odd-order capped reciprocal-Chebyshev transfer function (2a) and its associated center frequency NGD derived similarly as in [13] are, respectively, given by:

$$H_{1st}(j\omega) = \frac{\omega - j\Delta\omega_1}{\omega - j\Delta\omega_2}, \tag{4a}$$

$$\tau_{1st}(0) = -\frac{1}{\Delta\omega_1} + \frac{1}{\Delta\omega_2} = -\frac{1}{C_{\omega-3\,dB}}\left(\frac{1}{k_1} - \frac{1}{k_1'}\right). \tag{4b}$$

Similarly, the general form of the 2nd-order factorized rational function(s) present in any odd-order $N \geq 3$ capped reciprocal-Chebyshev transfer function (2a) and their associated center frequency NGD derived similarly as in [13] are, respectively, given by:

$$H_{2nd}(j\omega) = \frac{\omega^2 - j\Delta\omega_1\omega - \omega_{01}^2}{\omega^2 - j\Delta\omega_2\omega - \omega_{02}^2}, \tag{5a}$$

$$\tau_{2nd}(0) = -\frac{\Delta\omega_1}{\omega_{01}^2} + \frac{\Delta\omega_2}{\omega_{02}^2} = -\frac{1}{C_{\omega-3\,\text{dB}}}\left(\frac{2k_1\sin\left(\frac{2m-1}{N}\frac{\pi}{2}\right)}{k_1^2 + \cos^2\left(\frac{2m-1}{N}\frac{\pi}{2}\right)} - \frac{2k_1'\sin\left(\frac{2m-1}{N}\frac{\pi}{2}\right)}{k_1'^2 + \cos^2\left(\frac{2m-1}{N}\frac{\pi}{2}\right)}\right). \tag{5b}$$

The product of 1st and 2nd-order factorized functions in (2a) translates into a sum of center frequency NGD values given by (4b) and (5b). Therefore, the center frequency NGD value for odd-orders of the proposed capped reciprocal-Chebyshev design, corrected for 3 dB-bandwidth, is given by:

$$\tau_{odd}(0) = -\frac{1}{C_{\omega-3\,\text{dB}}}\left[\left(\frac{1}{k_1} - \frac{1}{k_1'}\right) + \sum_{m=1}^{(N-1)/2}\left(\frac{2k_1\sin\left(\frac{2m-1}{N}\frac{\pi}{2}\right)}{k_1^2+\cos^2\left(\frac{2m-1}{N}\frac{\pi}{2}\right)} - \frac{2k_1'\sin\left(\frac{2m-1}{N}\frac{\pi}{2}\right)}{k_1'^2+\cos^2\left(\frac{2m-1}{N}\frac{\pi}{2}\right)}\right)\right]. \tag{6}$$

In Fig. (2b) examples with $A = 100$ (40 dB), in-band ripple of $R_{\text{dB}} = 2$ dB, expression (6) in conjunction with expressions (2b)–(2d) yield center frequency NGD values, NGD $= -\tau(0) = 2.5909$ s, 3.6176 s, 4.3589 s, for $N = 3, 5, 7$, respectively. Since the corrected 3 dB-bandwidth cut-off frequency is $\omega_c = 1$, corresponding NGD-bandwidth product values are $\text{NGD}\cdot\Delta f = \text{NGD}\cdot\omega_c/\pi = 0.8247, 1.1515, 1.3875$, for $N = 3, 5, 7$, respectively. As a comparison, for the same out-of-band gain $A = 100$ (40 dB), capped reciprocal-Butterworth design [13] yields smaller values of $\text{NGD}\cdot\Delta f = 0.4995, 0.6200, 0.6896$, for $N = 3, 5, 7$, respectively.

3. BASEBAND NGD FILTER TRANSFORMATION TO BAND-STOP-FILTER (BSF)

The proposed capped reciprocal-Chebyshev transfer function given by (2a) can be transformed from the baseband form to its equivalent form centered at a non-zero center frequency ω_0. This equivalent BSF transfer function form (with a finite band-stop attenuation) is obtained via the same frequency substitution applied in a low-pass to bandpass filter transformation [13]:

$$\omega \to \frac{1}{2}\left(\omega - \frac{\omega_0^2}{\omega}\right). \tag{7}$$

When the transformation (7) is applied to the baseband 2nd-order factorized rational function(s) given by (5a), it yields the frequency up-shifted form given by [13]:

$$H_{BSF2}(j\omega) = \left(\frac{\omega^2 - j\Delta\omega_{1p}\omega - \omega_{01p}^2}{\omega^2 - j\Delta\omega_{2p}\omega - \omega_{02p}^2}\right)\cdot\left(\frac{\omega^2 - j\Delta\omega_{3p}\omega - \omega_{03p}^2}{\omega^2 - j\Delta\omega_{4p}\omega - \omega_{04p}^2}\right). \tag{8}$$

The BSF transfer function (8) is given in its factorized form as a product of two 2nd-order rational functions, which is more suitable for subsequent circuit design as discussed in [10, 13].

From the four baseband frequency parameters in (5a), all eight frequency parameters in expression (8) can be determined from expressions reported in [10]. A few relationships between

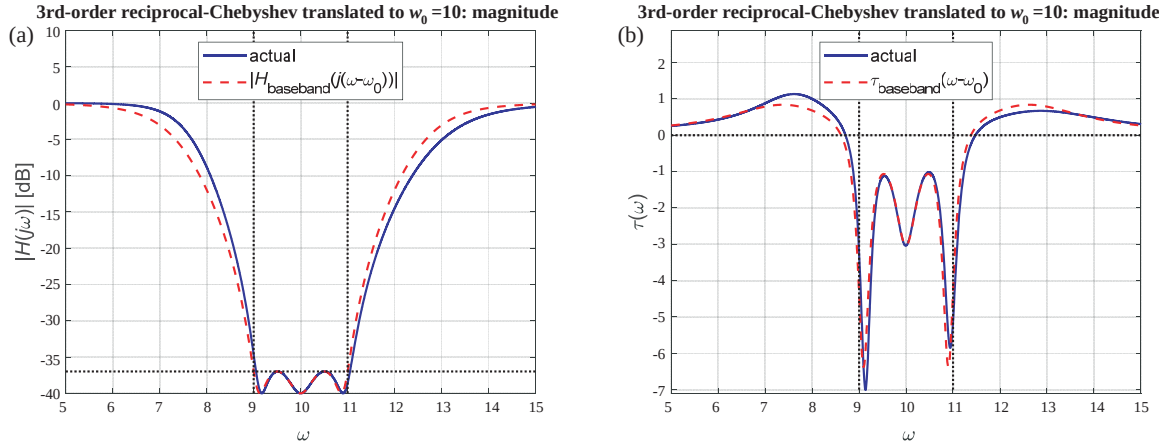

FIGURE 5. Example 3rd-order capped reciprocal-Chebyshev transfer function (a) magnitude and (b) group delay responses transformed to $\omega_0 = 10\omega_c = 10$ center frequency and compared with corresponding ideally translated baseband responses.

parameters in (8), selected for referencing purposes, are given by [10, 13]:

$$\omega_{03p} = \frac{\omega_0^2}{\omega_{01p}}, \quad \Delta\omega_{3p} = \frac{\omega_0^2}{\omega_{01p}^2}\Delta\omega_{1p} = \frac{\omega_{03p}}{\omega_{01p}}\Delta\omega_{1p}. \tag{9}$$

The geometric mean of the two 2nd-order rational transfer functions numerator's parameters ω_{01p} and ω_{03p} corresponds to the BSF center frequency ω_0, as noted from (9). Further, for the two numerator functions the quality factors are the same, $\omega_{01p}/\Delta\omega_{1p} = \omega_{03p}/\Delta\omega_{3p}$. For the corresponding denominator parameters, similar relationships to (9) apply with indices 2 and 4 replacing 1 and 3, respectively [10, 13].

When the transformation (7) is applied to the baseband 1st-order factorized rational function(s) given by (4a), it yields the frequency up-shifted form given by [13]:

$$H_{BSF1}(j\omega) = \frac{\omega^2 - j\Delta\omega_{5p}\omega - \omega_0^2}{\omega^2 - j\Delta\omega_{6p}\omega - \omega_0^2}, \tag{10}$$

where $\Delta\omega_{5p} = 2\Delta\omega_1$ and $\Delta\omega_{6p} = 2\Delta\omega_2$.

As an example, consider a 3rd-order capped reciprocal-Chebyshev baseband transfer function given by (3b), with an in-band ripple of $R_{\text{dB}} = 3\,\text{dB}$ ($\varepsilon = 1$) and out-of-band gain $A = 100$, or 40 dB (gain-uncompensated variation, divided by A):

$$H_{BB3-3\,\text{dB}}(j\omega) = \left(\frac{\omega - j\cdot 0.2980}{\omega - j\cdot 2.8385}\right) \cdot \left(\frac{\omega^2 - j\cdot 0.2980\omega - 0.9159^2}{\omega^2 - j\cdot 2.8385\omega - 2.9677^2}\right). \tag{11}$$

Employing expression (7), the frequency up-shift to $\omega_0 = 10\omega_c = 10$ chosen in this example yields (after factorization):

$$H_{BSF3}(j\omega) = \frac{\omega^2 - j0.5961\omega - 10^2}{\omega^2 - j5.6770\omega - 10^2} \cdot \left(\frac{\omega^2 - j0.3249\omega - 10.9445^2}{\omega^2 - j3.5608\omega - 12.9716^2}\right) \cdot \left(\frac{\omega^2 - j0.2712\omega - 9.1370^2}{\omega^2 - j2.1162\omega - 7.7092^2}\right). \tag{12}$$

The plots in Figs. 5(a) and 5(b) depict transfer function (12) magnitude and group delay characteristics, respectively, with out-of-band gain $A = 40\,\text{dB}$, $R_{\text{dB}} = 3\,\text{dB}$ in-band ripple, and normalized bandwidth $\Delta\omega = 2\omega_c = 2$. Comparing responses associated with (12) with the baseband ones (expression (11) ideally translated with $\omega \to \omega - \omega_0$) reveals a close in-band match in Figs. 5(a) and 5(b). Transfer function (12) achieves a center frequency NGD of 3.036 s or an NGD-bandwidth product of $NGD \cdot \Delta f = 0.9664$ (the same as the corresponding baseband transfer function).

Note that the numerators of two 2nd-order rational functions in (12), associated with translating the single 2nd-order baseband rational function in (11), have resonant frequencies (10.9445 and 9.1370) which are different from those in the denominators (12.9716 and 7.7092). However, the product of the numerator frequency parameters is the same as the product associated with denominator parameters ($10.9445 \times 9.1370 = 12.9716 \times 7.7092 = \omega_0^2 = 100$). This is congruent with the geometric mean property in (9) and also yields the required constant out-of-band gain A on both sides relative to the center frequency magnitude response. This is corroborated by Fig. 5(a), as well as by evaluating expression (12) at the center frequencies and out-of-band extremes ($H(0) = 1$, $H(\omega \to \infty) = 1$, $H(\omega_0) = 1/A$).

4. EXACT IMPLEMENTATION WITH SALLEN-KEY TOPOLOGY

A Sallen-Key topology depicted in Fig. 6 schematic can implement a 3rd-order baseband capped reciprocal-Chebyshev transfer function upshifted to higher center frequency ω_0, which yields an overall 6th-order BSF transfer function such as (12). Cascaded versions of the topology in Fig. 6 can achieve higher order capped reciprocal-Chebyshev designs, similar to capped reciprocal-Butterworth designs detailed in [13]. Given the system impedance Z_0, transfer function of Fig. 6 topology and its

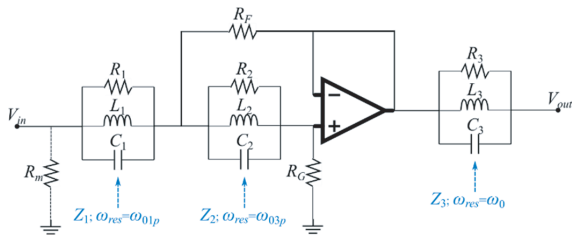

FIGURE 6. Sallen-Key topology that can be used to achieve an exact 3rd-order capped reciprocal-Chebyshev baseband NGD transfer function translated to a higher center frequency ω_0 (BSF).

input impedance are given by, respectively [13]:

$$H(j\omega) = \frac{V_{out}}{V_{in}} = \frac{R_G \cdot R_F}{R_G \cdot R_F + Z_1 \cdot Z_2 + R_F \cdot (Z_1 + Z_2)} \frac{Z_0}{Z_0 + Z_3}, \quad (13)$$

$$Z_{in} = \frac{R_G \cdot R_F + Z_1 \cdot Z_2 + R_F \cdot (Z_1 + Z_2)}{R_F + Z_2}. \quad (14)$$

Expression (12), associated with an overall 6th-order capped reciprocal-Chebyshev BSF function is used for a Fig. 6 topology implementation example. An out-of-band gain $A = 100$ (40 dB) was chosen, $R_{\text{dB}} = 3$ dB ripple, and 3-dB cut-off frequency $\omega_c = \Delta\omega/2$ related to the center frequency as $\omega_0 = 10\omega_c$. Transfer function (12) parameters are summarized as:

$$\begin{aligned} \omega_{01p} &= 10.9445\omega_c, \quad \Delta\omega_{1p} = 0.3249\omega_c, \\ \omega_{03p} &= 9.137\omega_c, \quad \Delta\omega_{3p} = 0.2712\omega_c, \quad (15a) \\ \omega_{02p} &= 12.9716\omega_c, \quad \Delta\omega_{2p} = 3.5608\omega_c, \\ \omega_{04p} &= 7.7092\omega_c, \quad \Delta\omega_{4p} = 2.1162\omega_c, \quad (15b) \\ \omega_0 &= 10\omega_c, \quad \Delta\omega_{5p} = 0.5961\omega_c, \\ \Delta\omega_{6p} &= 5.677\omega_c. \quad (15c) \end{aligned}$$

The BSF transfer function (12) with parameters given by (15a)–(15c) can be equated to the Sallen-Key transfer function (13), to solve for component values depicted in Fig. 6 [13]. For a chosen bandwidth of $\Delta f = 2f_c = 100$ MHz, center frequency $f_0 = 10f_c = 500$ MHz, input impedance at center frequency $Z_{in} \approx 40Z_0 = 2$ kΩ, Fig. 6 component values can be calculated as [10, 13]:

$$R_1 \approx Z_{in} = 2\,\text{k}\Omega, \quad C_1 = \frac{1}{\Delta\omega_{1p}R_1} = 4.899\,\text{pF},$$

$$L_1 = \frac{1}{\omega_{01p}^2 C_1} = 17.266\,\text{nH}, \quad (16a)$$

$$R_2 = R_1 = 2\,\text{k}\Omega, \quad C_2 = \frac{1}{\Delta\omega_{3p}R_2} = 5.868\,\text{pF},$$

$$L_2 = \frac{1}{\omega_{03p}^2 C_2} = 20.681\,\text{nH}, \quad (16b)$$

$$R_G = \frac{1/C_1 + 1/C_2}{\Delta\omega_{2p} + \Delta\omega_{4p} - \Delta\omega_{1p} - \Delta\omega_{3p}} = 234.6\,\Omega, \quad (16c)$$

$$R_F = \frac{1}{(\omega_{02p}^2 + \omega_{04p}^2 + \Delta\omega_{2p}\Delta\omega_{4p} - \omega_{01p}^2 - \omega_{03p}^2 - \Delta\omega_{1p}\Delta\omega_{3p})R_G C_1 C_2 - \frac{2}{R_1^2}} = 49.455\,\Omega, \quad (16d)$$

$$R_3 = Z_0\,(\Delta\omega_{6p}/\Delta\omega_{5p} - 1) = 426.21\,\Omega,$$

$$C_3 = \frac{1}{\Delta\omega_{5p}R_3} = 12.529\,\text{pF},$$

$$L_3 = \frac{1}{\omega_0^2 C_3} = 8.087\,\text{nH}. \quad (16e)$$

Tuned frequencies of the two resonators at the op-amp input of the topology in Fig. 6 in this case are $f_{01p} = 10.9445f_c = 547.23$ MHz, and $f_{03p} = 9.137f_c = 456.85$ MHz, as given by (15a). The remaining 2nd-order term in (12) tuned at the overall design center frequency $f_0 = 500$ MHz is implemented with a resonator at the op-amp output shown in Fig. 6, and its component values are calculated by (16e). Fig. 7 shows transfer function magnitude and group delay responses of Fig. 6 topology, for an ideal source design, as well as a design with a matching shunt input resistor $R_m = 51.28\,\Omega$, driven by a 50 Ω-source [13].

For the ideal-source and resistor-matched designs, the center frequency NGD values are 9.66 ns and 9.45 ns, and the 3 dB-bandwidths are 100 MHz and 100.5 MHz, yielding the NGD-bandwidth products of 0.9664 and 0.9495, respectively. Sensitivity analysis results for the component values of this design are similar to those for the corresponding capped reciprocal-Butterworth circuit described in [13]. The presented design is mostly intended as a proof-of-concept in this paper.

5. APPROXIMATE IMPLEMENTATION WITH PASSIVE LADDER CIRCUIT TOPOLOGY

A Sallen-Key topology discussed in the previous section can implement the exact BSF capped reciprocal-Chebyshev design transfer function, such as (12). However, it comes at a cost of employing op-amps (for odd-Nth order, $(N-1)/2$ op-amps are needed). Further, op-amp(s) in this topology do not provide gain-compensation, so the design has an attenuation at the center frequency as evident from Fig. 7(a), just like a purely passive NGD topology would have.

Alternatively, a relatively good match to the exact BSF transfer function can be achieved with an all-passive ladder topology involving resonators, such as a π-circuit illustrated in Fig. 8 [13]. An alternative T-circuit equivalent of this topology is discussed in [13]. Assuming a Z_0-impedance source and load, transfer function of the Fig. 8 design is given by [13]:

$$H(j\omega) = \frac{V_{out}}{V_{in}} = \frac{2}{(1 + Z_2/Z_0 + Z_2/Z_3) \cdot (1 + Z_0/Z_1) + (1 + Z_0/Z_3)}. \quad (17)$$

The BSF transfer function (12) with parameters given by (15a)–(15c) can be equated to transfer function (17), in an attempt to solve for component values depicted in Fig. 8 [13]. After frequency-dependent impedance expressions are substituted in (17), the overall transfer function can be factorized into three

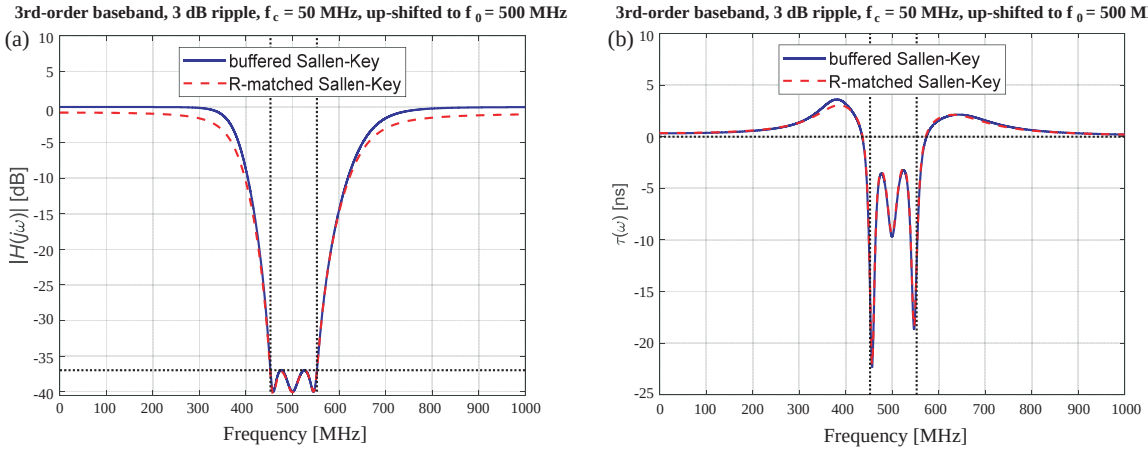

FIGURE 7. Transmission coefficient (a) and group delay (b) of the ideal source (buffered) driven Sallen-Key design, and of the shunt resistor matched design driven by a 50 Ω source, for the BSF capped reciprocal-Chebyshev transfer function.

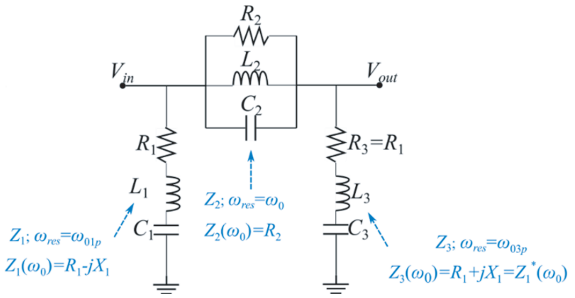

FIGURE 8. Three-resonator π-circuit ladder topology that can achieve an approximate 3rd-order baseband capped reciprocal-Chebyshev NGD transfer function translated to a higher center frequency ω_0 (BSF).

2nd-order rational functions to have the same form as (12). The numerators of the exact BSF transfer function (12) and the π-circuit transfer function (17) after impedance expressions are expanded can be exactly matched [13], and are given by:

$$\begin{aligned} \omega_{01p} &= \omega_{01\pi} = 10.9445\omega_c, \\ \Delta\omega_{1p} &= \Delta\omega_{1\pi} = 0.3249\omega_c, \\ \omega_{03p} &= \omega_{03\pi} = 9.137\omega_c, \\ \Delta\omega_{3p} &= \Delta\omega_{3\pi} = 0.2712\omega_c, \\ \omega_{05p} &= \omega_{05\pi} = \omega_0 = 10\omega_c, \\ \Delta\omega_{5p} &= \Delta\omega_{5\pi} = 0.5961\omega_c. \end{aligned} \tag{18}$$

Further, as shown in [13], shunt impedances Z_1 and Z_3 need to be complex conjugates of each other at ω_0, in order to satisfy the required center frequency transfer function value of $H(j\omega_0) = 1/A$. Additionally, analysis detailed in [13] showed that the middle resonator resistor value in Fig. 8 can be calculated as:

$$R_2 = 2\frac{(A-1)\left(R_1^2+X_1^2\right) - Z_0R_1}{\left(R_1^2+X_1^2\right)/Z_0 - 2R_1 + Z_0} \tag{19}$$

where X_1 is the reactance of shunt resonators at ω_0, as labeled in Fig. 8. From (19), given the $R_1 = R_3$ requirement, the only degree of freedom of this design then becomes the shunt resonators' resistance value R_1. Therefore, an exact match of transfer functions (17) and (12) is not possible, but an in-band match optimization can be used [13].

Since a characteristic of Chebyshev filters is an in-band rippled magnitude response, its center frequency curvature (2nd derivative) closest to one of the exact transfer function (12) is used to determine the optimal value R_1. In this example with out-of-band gain $A = 100$ (40 dB) and $R_{\text{dB}} = 3$ dB in-band ripple, an optimal value $R_1 = 2.5945\,\Omega$ is obtained. Such optimized denominator parameters of the π-circuit transfer function (17), along with the exact ones in (12), are:

$$\begin{aligned} \omega_{02\pi} &= 12.8198\omega_c, \quad \Delta\omega_{2\pi} = 3.7111\omega_c, \\ \omega_{04\pi} &= 7.8004\omega_c, \quad \Delta\omega_{4\pi} = 2.2581\omega_c, \end{aligned} \tag{20a}$$

$$\begin{aligned} \omega_{02p} &= 12.9716\omega_c, \quad \Delta\omega_{2p} = 3.5608\omega_c, \\ \omega_{04p} &= 7.7092\omega_c, \quad \Delta\omega_{4p} = 2.1162\omega_c, \end{aligned} \tag{20b}$$

$$\begin{aligned} \Delta\omega_{6\pi} &= 5.9568\omega_c, \quad \Delta\omega_{6p} = 5.677\omega_c, \\ \omega_{06\pi} &= \omega_{06p} = \omega_0 = 10\omega_c. \end{aligned} \tag{20c}$$

Substituting the optimized $R_1 = 2.5945\,\Omega$ value, out-of-band gain $A = 100$ (40 dB), system impedance $Z_0 = 50\,\Omega$, and the center frequency reactance magnitude of the shunt branches in Fig. 8, $X_1 = (1/(\omega_0 C_1) - \omega_0 L_1) = 15.7993\,\Omega$, into expression (19) yields $R_2 = 837.2241\,\Omega$. All component values corresponding to the design in Fig. 8 in this example are then given by:

$$\begin{aligned} R_1 &= 2.5945\,\Omega, \quad L_1 = \frac{1}{\Delta\omega_{1p}R_1} = 25.422\,\text{nH}, \\ C_1 &= \frac{1}{\omega_{01p}^2 L_1} = 3.3273\,\text{pF}, \end{aligned} \tag{21a}$$

$$\begin{aligned} R_3 &= 2.5945\,\Omega, \quad L_3 = \frac{1}{\Delta\omega_{3p}R_3} = 30.4511\,\text{nH}, \\ C_3 &= \frac{1}{\omega_{03p}^2 L_3} = 3.9856\,\text{pF}, \end{aligned} \tag{21b}$$

$$R_2 = 837.2241\,\Omega, \quad C_2 = \frac{1}{2\omega_c R_2} = 6.3784\,\text{pF},$$

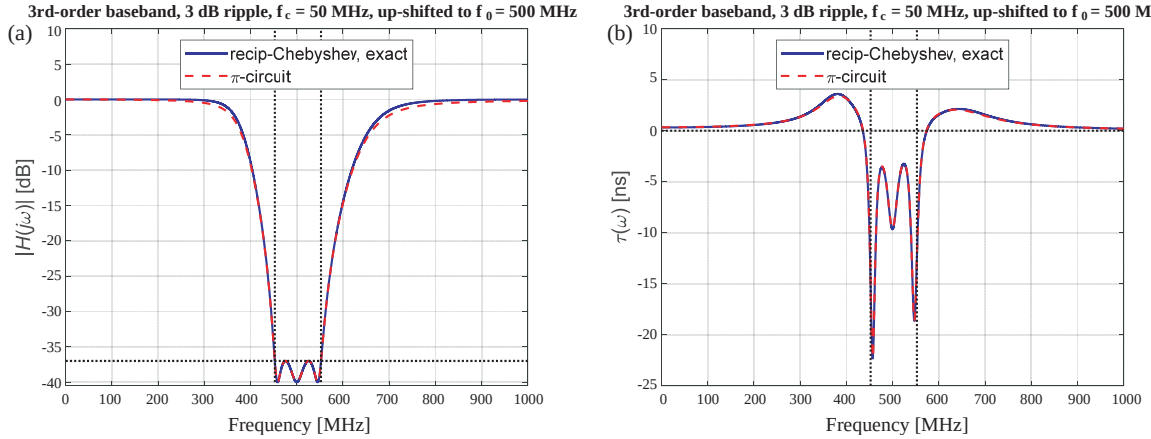

FIGURE 9. Transfer function magnitude (a) and group delay (b) responses of the exact capped reciprocal-Chebyshev 3rd-order design upshifted to a higher center frequency, and of the π-circuit all-passive design.

$$L_2 = \frac{1}{\omega_0^2 C_2} = 15.8849\,\text{nH}. \tag{21c}$$

Figure 9 shows the transfer function magnitude and group delay responses of Fig. 8 topology. The center frequency NGD values are 9.66 ns and 9.61 ns, for the exact and π-circuit designs, respectively.

Sensitivity analysis results for the component values of this design are similar to those for the corresponding capped reciprocal-Butterworth circuit described in [13]. The component sensitivity is higher than corresponding bandpass filter of the same order, and the presented design is mostly intended as a proof-of-concept in this paper. Higher order capped reciprocal-Chebyshev passive ladder topology designs can be implemented by following the method described for capped reciprocal-Butterworth designs in [13].

6. NGD-BANDWIDTH PRODUCT ASYMPTOTIC LIMIT OF AN *N*TH-ORDER CAPPED RECIPROCAL-CHEBYSHEV DESIGN

Similar to the capped reciprocal-Butterworth design [13], the NGD-bandwidth product of the Nth-order capped reciprocal-Chebyshev design can be expressed as a function of the trade-off quantity, out-of-band gain. An upper asymptotic limit of this functional relationship can be found, as the design order becomes large. For the capped reciprocal-Butterworth NGD design in [13], the NGD-bandwidth asymptotic limit was shown to be a linear function of the out-of-band gain in decibels, approximately equal to $0.0233 \cdot A_{\text{dB}}$.

From the center frequency NGD expressions (6), odd Nth-order baseband capped reciprocal-Chebyshev designs have an NGD-bandwidth product given by:

$$NGD \cdot \Delta f = -\tau(0) \cdot \frac{2\omega_c}{2\pi} = \frac{1}{\pi} \frac{1}{C_{\omega-3\,\text{dB}}} \left[\left(\frac{1}{k_1} - \frac{1}{k_1'} \right) + \sum_{m=1}^{(N-1)/2} \left(\frac{2k_1 \sin\left(\frac{2m-1}{N}\frac{\pi}{2}\right)}{k_1^2 + \cos^2\left(\frac{2m-1}{N}\frac{\pi}{2}\right)} - \frac{2k_1' \sin\left(\frac{2m-1}{N}\frac{\pi}{2}\right)}{k_1'^2 + \cos^2\left(\frac{2m-1}{N}\frac{\pi}{2}\right)} \right) \right]. \tag{22}$$

Further, employing the trapezoidal area sum approximation for an integral evaluation, the first part of the sum from (22) can be approximated as (for odd orders $N \geq 7$, yielding at least three sum terms):

$$\sum_{m=1}^{(N-1)/2} \frac{2k_1 \sin\left(\frac{2m-1}{N}\frac{\pi}{2}\right)}{k_1^2 + \cos^2\left(\frac{2m-1}{N}\frac{\pi}{2}\right)} \approx \frac{2N}{\pi} \int_{\pi/(2N)}^{\pi(N-2)/(2N)} \frac{k_1 \sin(x)}{k_1^2 + \cos^2(x)} dx + \frac{k_1 \sin\left(\frac{\pi}{2N}\right)}{k_1^2 + \cos^2\left(\frac{\pi}{2N}\right)} + \frac{k_1 \cos\left(\frac{\pi}{N}\right)}{k_1^2 + \sin^2\left(\frac{\pi}{N}\right)}, \tag{23a}$$

where the resulting integral can be solved in a closed form:

$$\int \frac{k_1 \sin(x)}{k_1^2 + \cos^2(x)} dx = -\tan^{-1}\left(\frac{\cos(x)}{k_1}\right). \tag{23b}$$

Similar expression to (23a) can be obtained for the second part of the sum in (22), involving k_1'. For a large design order N, using small argument approximations for $\sinh(x) \approx x$, $\cosh(x) \approx 1$, and a large argument approximation for $\tan^{-1}(y) \approx \pi/2 - 1/y$, NGD-bandwidth product asymptotic expression for capped reciprocal-Chebyshev design can be derived as:

$$NGD \cdot \Delta f \approx \frac{\ln(10)}{10 \cdot \pi^2} \cdot A_{\text{dB}} + N \cdot \frac{1}{\pi} \left(\frac{1}{\sinh^{-1}\left(\frac{1}{\varepsilon}\right)} - \frac{2}{\pi} \tan^{-1}\left(\frac{\pi}{\sinh^{-1}\left(\frac{1}{\varepsilon}\right)} \right) \right.$$

$$+\frac{1}{\sinh^{-1}\left(\frac{1}{\varepsilon}\right)+\frac{\pi^2}{\sinh^{-1}\left(\frac{1}{\varepsilon}\right)}}\Bigg)$$

$$+\frac{2}{\pi^2}\cdot\left(\ln\left(\frac{2}{\varepsilon}\right)-\sinh^{-1}\left(\frac{1}{\varepsilon}\right)\right). \quad (24)$$

The first term in expression (24), proportional to decibel value of out-of-band gain and approximately yielding $0.0233\cdot A_{\text{dB}}$, is identical to the NGD-bandwidth asymptotic expression of the capped reciprocal-Butterworth design [13]. The additional "offset" term in the capped reciprocal-Chebyshev asymptotic NGD-bandwidth expression (24) is approximated by a linear function of the odd-order number N, representing an NGD-bandwidth improvement over the capped reciprocal-Butterworth design.

Expression (24), applicable to large values of odd-order numbers N, for selected in-band ripple amplitude values yields:

$$(NGD\cdot\Delta f)_{3\text{ dB-}ripple} \approx 0.0233\cdot A_{\text{dB}}+(0.1246\cdot N-0.0381). \quad (25a)$$

$$(NGD\cdot\Delta f)_{1\text{dB-}ripple} \approx 0.0233\cdot A_{\text{dB}}+(0.0292\cdot N-0.0120). \quad (25b)$$

$$(NGD\cdot\Delta f)_{0.5\text{ dB-}ripple} \approx 0.0233\cdot A_{\text{dB}}+(0.0087\cdot N-0.0059). \quad (25c)$$

Expressions (25a)–(25c) demonstrate that the asymptotic NGD-bandwidth offset as a linear function of an odd-order N is also proportional to the in-band ripple magnitude. The NGD-bandwidth product for several odd-order baseband capped reciprocal-Chebyshev designs, as a function of out-of-band gain, is plotted in Fig. 10 based on expression (24).

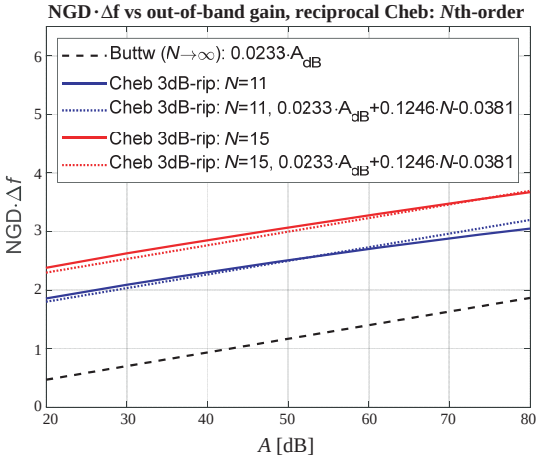

FIGURE 10. Asymptotic NGD-bandwidth product for large odd-order baseband capped reciprocal-Chebyshev designs, as a function of overall out-of-band gain.

7. RELATIONSHIP BETWEEN TIME DOMAIN AND FREQUENCY DOMAIN NGD METRICS

The transient's magnitude amplification phenomenon exhibited in NGD designs is proportional to the out-of-band gain, as discussed in detail in [13]. It is also demonstrated here for a Gaussian pulse example with finite turn-on/off times, propagated through selected capped reciprocal-Chebyshev and capped reciprocal-Butterworth NGD designs.

Both example designs are chosen to be of 5th-order, have an out-of-band gain of 40 dB ($A = 100$) and are gain-compensated at the center frequency (0 dB), with capped reciprocal-Chebyshev design having a 0.5 dB in-band ripple amplitude. The input Gaussian pulse chosen in this example is the same as the one detailed in [13], with its frequency spectrum standard deviation related to the 3 dB-bandwidth cut-off frequency as $\sigma_\omega = \omega_c/3 = 1/3$, and its turn-on/off times selected at $3.5\sigma_t$ ($\sigma_t = 1/\sigma_\omega$). The compared 5th-order, 40 dB out-of-band gain, capped reciprocal-Butterworth and capped reciprocal-Chebyshev (with a 0.5 dB in-band ripple) designs have NGD-bandwidth product values of $NGD\cdot\Delta f = 0.62$, and 0.8226, respectively, which for a bandwidth of $\Delta f = \omega_c/\pi = 1/\pi$ yield center frequency NGD values of 1.948 s and 2.584 s, respectively. The corresponding time domain Gaussian pulse-peak advancement values in Fig. 11(b) are comparable at 2.146 s and 2.565 s, respectively, as expected. Further, transient amplitudes observed in Fig. 11(b) are practically the same for the two designs, which is expected due to their identical out-of-band gains [13].

Figure 12 shows NGD-bandwidth product variation with out-of-band gain for selected capped reciprocal-Chebyshev and capped reciprocal-Butterworth designs, with both frequency domain values and time domain values corresponding to time-advancement of a Gaussian pulse peak. Fig. 12 shows that for the capped reciprocal-Butterworth design the time domain NGD is higher than the frequency domain value, and vice versa for capped reciprocal-Chebyshev designs. Further, for capped reciprocal-Chebyshev designs the frequency domain NGD keeps increasing with the in-band ripple amplitude, whereas the time-domain NGD shows only a marginal increase after 0.5 dB ripple, in this case. This phenomenon puts a practical limit on the in-band ripple amplitude of the capped reciprocal-Chebyshev designs, due to diminishing time-domain NGD increase and a considerable distortion increase at the same time, as it will be discussed in the next section.

8. IN-BAND COMBINED MAGNITUDE/PHASE RESPONSE DISTORTION METRIC

Performances of different NGD designs can be quantified and compared based on a Figure of Merit (FOM) metric, such as the one reported in [10, 13]:

$$FOM = \frac{NGD\cdot BW}{A_{\text{dB}}}. \quad (26)$$

FOM in expression (26) is defined as a ratio of the achieved NGD-bandwidth product, and the undesired trade-off quantity, out-of-band gain. One of the undesired properties of the out-of-band gain is its proportional relationship to transients associated with information carrying signals, as demonstrated in Section 7 and also discussed in [8–10, 13]. For waveforms where there is no transients concern and the focus is on gain-compensation, the FOM expression (26) can be modified to

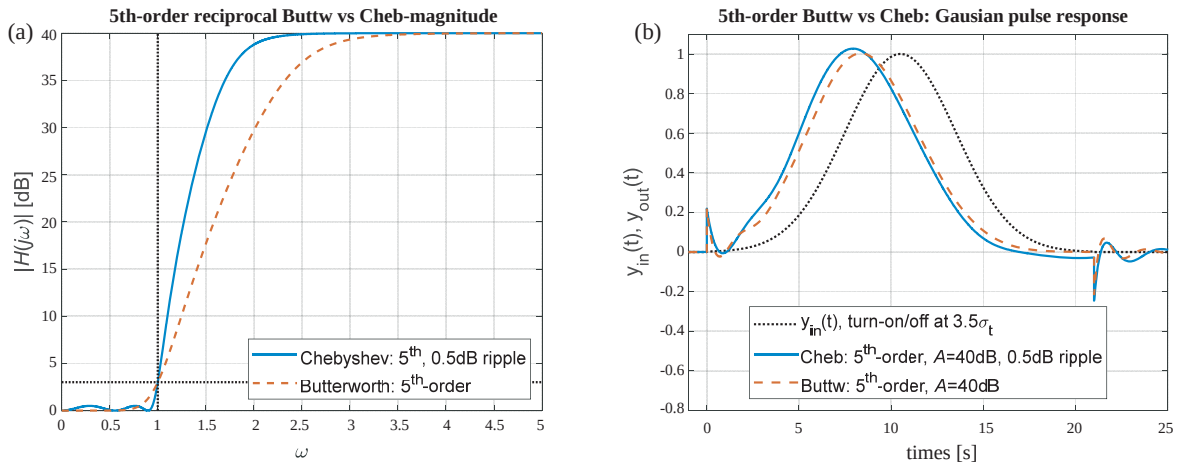

FIGURE 11. 5th-order, 40 dB out-of-band gain capped reciprocal-Butterworth and capped reciprocal-Chebyshev (0.5 dB in-band ripple) baseband designs (a) magnitude responses, and (b) time-domain responses to a Gaussian pulse turned-on/off at $3.5\sigma_t$.

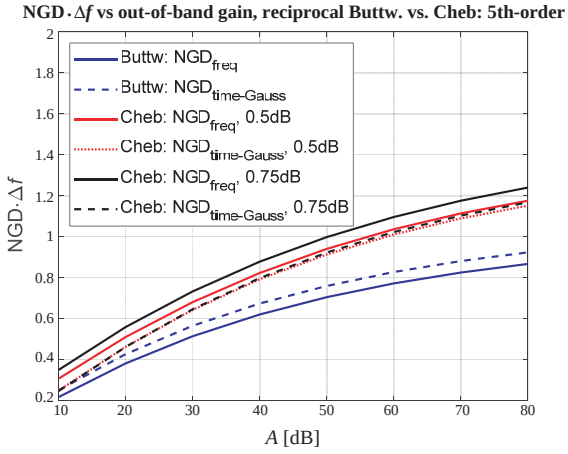

FIGURE 12. NGD-bandwidth product as a function of out-of-band gain for selected 5th-order capped reciprocal-Chebyshev and capped reciprocal-Butterworth designs, with frequency domain, and corresponding time domain NGD for an applied Gaussian pulse.

replace the $1/A_{\text{dB}}$ term by the center frequency magnitude response value, $|H(j\omega_0)|$.

Another NGD trade-off is a distortion associated with variations in the magnitude response, as well as variations in the group delay characteristic (phase non-linearity), within the in-band (typically 3 dB-bandwidth). For waveforms with associated transients, this in-band combined magnitude/phase distortion affects the "steady-state" part of the waveform which follows any transient settling [13]. Waveforms with no associated transients are also affected by the in-band distortion.

The in-band distortion will affect applied waveforms differently, based on their frequency spectrums. A distortion metric for an NGD baseband transfer function $H(j\omega)$, an input waveform $f(t)$ and its frequency spectrum $F(j\omega)$, observed time-domain advancement of the output waveform peak Δt_{pk}, input/output pulse peak magnitudes $f_{\max}/y_{\max}$, and a 3 dB cut-off ω_c is given by [13]:

$$D_{in\text{-}band} = \sqrt{\frac{\int_0^{\omega_c} |F(j\omega) - e^{-j\omega\Delta t_{pk}} F(j\omega)H(j\omega)\cdot f_{\max}/y_{\max}|^2 d\omega}{\int_0^{\omega_c} |F(j\omega)|^2 d\omega}}. \quad (27)$$

As an example, the distortion metric is examined for a Gaussian pulse input waveform (NGD 3 dB-bandwidth comprises 6 standard deviations of the pulse frequency spectrum) applied to a 5th-order capped reciprocal-Chebyshev design with a chosen out-of-band gain $A = 40$ dB and in-band ripple of 0.5 dB. Fig. 13 depicts input and output waveforms, and the distortion metric calculated from (27) is $D_{\text{in-band-Gaussian}} = 0.0413$. As a reference, $D_{\text{low-pass-Gaussian}} = 0.0411$, for a classical 1st-order low-pass filter. The center frequency NGD of the capped reciprocal-Chebyshev design is $-\tau(0) = 2.584$ s, yielding an NGD-bandwidth product of 0.8226, as shown in Fig. 12. This is somewhat higher but comparable to the time domain advancement of the pulse depicted in Fig. 13, where $\Delta t_{pk} = 2.488$ s (congruent with Fig. 12 trend between frequency and time-domain NGD).

NGD-bandwidth product (NGD as observed in the time domain) as a function of out-of-band gain is shown in Fig. 14 for selected 5th-order capped reciprocal-Chebyshev designs. Solid curves in Fig. 14 are associated with a 3 dB-bandwidth, while dashed curves are associated with a reduced bandwidth needed to keep the distortion metric below the chosen reference 1st-order low-pass filter value ($D = 0.0411$ for a Gaussian pulse). Corresponding capped reciprocal-Butterworth case [13] is shown as well in Fig. 14, as a reference.

It can be noted from Fig. 14 that the NGD-bandwidth product is higher for the 0.75 dB than the 0.5 dB in-band ripple case when distortion is ignored, i.e., input bandwidth kept at medium's 3 dB cut-off frequency in both cases (solid curves). However, with the two inputs' respective bandwidths reduced to yield the distortion metric below that of a 1st-order low-pass

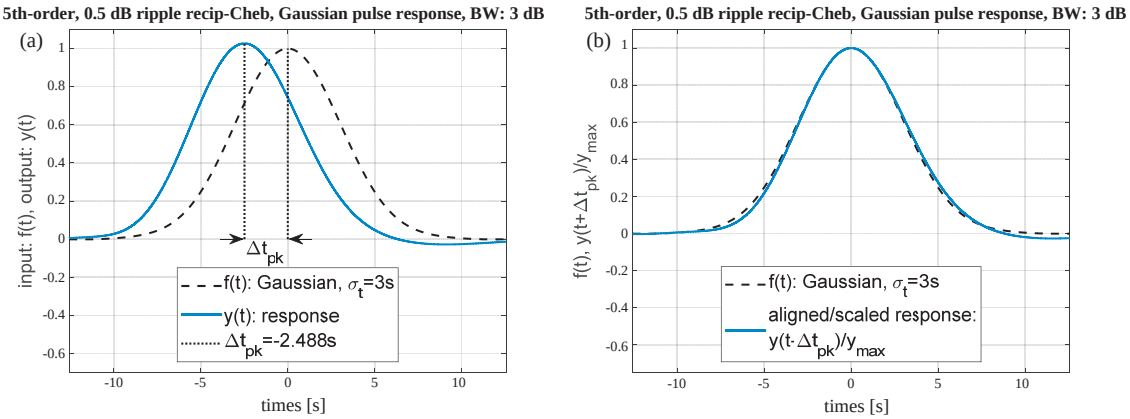

FIGURE 13. (a) Input Gaussian pulse with a frequency spectrum cut-off at $\omega_c = 1$, and the corresponding output waveform for a 5th-order capped reciprocal-Chebyshev gain-compensated design. (b) The same comparison but with the output waveform shifted by Δt_{pk} and normalized by $|y(t)|_{\max}$.

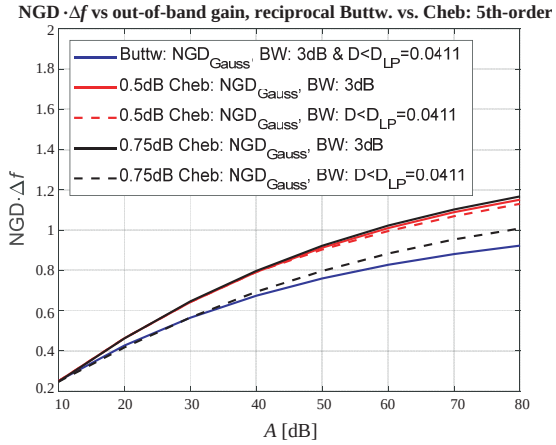

FIGURE 14. NGD-bandwidth product (using time domain NGD) for a Gaussian input applied to selected 5th-order designs with 3-dB bandwidth (solid curves) vs. reduced bandwidth yielding the same distortion metric as a 1st-order low-pass filter ($D_{LP} = 0.0411$).

filter, the Gaussian pulse time domain NGD-bandwidth product for the 0.5 dB in-band ripple case is now higher than the 0.75 dB one. This demonstrates that reducing the medium's effective bandwidth below the 3 dB cut-off frequency is not as effective for capped reciprocal-Chebyshev designs, when the presented distortion metric is considered. Reducing the in-band ripple and/or the design order is recommended instead.

Input and output waveform cross-correlation [26, 30] is a complementary distortion metric to the one given by (27), roughly related as a square root of $1 - D^2$. It should be kept in mind, however, that seemingly high cross-correlation numbers can still be associated with a high distortion metric (for example, correlation of 0.95 roughly yields a distortion of $D = 0.312$). Another combined magnitude/phase distortion metric of an NGD medium is presented in [33], which is used to define an NGD bandwidth with an acceptable level of distortion. The main difference to the metric given by (27) is that the metric from [33] considers the medium only, without the specific applied waveform consideration.

When an in-band distortion limit is imposed on an NGD design, it is assumed that the objective is to maintain reasonable input/output waveform fidelity. Alternatively, in NGD design applications targeting magnitude/phase (group delay) equalization of the preceding stage transfer function, distortion metric presented in [13], and in this paper, can be evaluated for the overall design including the preceding stage(s).

9. IMPLICATIONS OF USING THE ENTIRE BANDWIDTH WHERE GROUP DELAY IS NEGATIVE

Group delay response is negative over a frequency bandwidth $\tau(\omega) < 0$, which in many NGD designs can be considerably wider than the 3 dB-bandwidth, as discussed in [13]. In many NGD publications, the $\tau(\omega) < 0$ defined bandwidth is reported as the actual design bandwidth, and as such used in performance metrics instead of the typically smaller 3 dB-bandwidth. However, if the $\tau(\omega) < 0$ defined bandwidth is not validated with input waveforms corresponding to that bandwidth, it can result in unacceptably high distortion of associated output waveforms, as also discussed in [33].

Group delay response zero-crossings for a capped reciprocal-Butterworth design can be solved for analytically [13], showing that $\tau(\omega) < 0$ bandwidth approximately corresponds to magnitude response variation equal to the half of the out-of-band gain in decibels, $A_{\text{dB}}/2$.

Capped reciprocal-Chebyshev design presented in this paper does not yield such a concise explicit solution for group delay response zero-crossings, but in general it yields a smaller $\tau(\omega) < 0$ to 3 dB-bandwidth ratio than capped reciprocal-Butterworth design presented in [13]. For example, a 5th-order capped reciprocal-Chebyshev design with 40 dB out-of-band gain and a 0.5 dB in-band ripple yields a $\tau(\omega) < 0$ to 3 dB-bandwidth ratio of 1.203 (as corroborated in Fig. 4(b)). This yields a distortion metric from expression (27) of 0.1121 for a Gaussian waveform (2.73 times higher than distortion metric of a 1st-order low-pass filter, used as reference). Further, the in-band magnitude variation for $\tau(\omega) < 0$ bandwidth is somewhat less than $A_{\text{dB}}/2 = 20$ dB, as corroborated in Fig. 4(a).

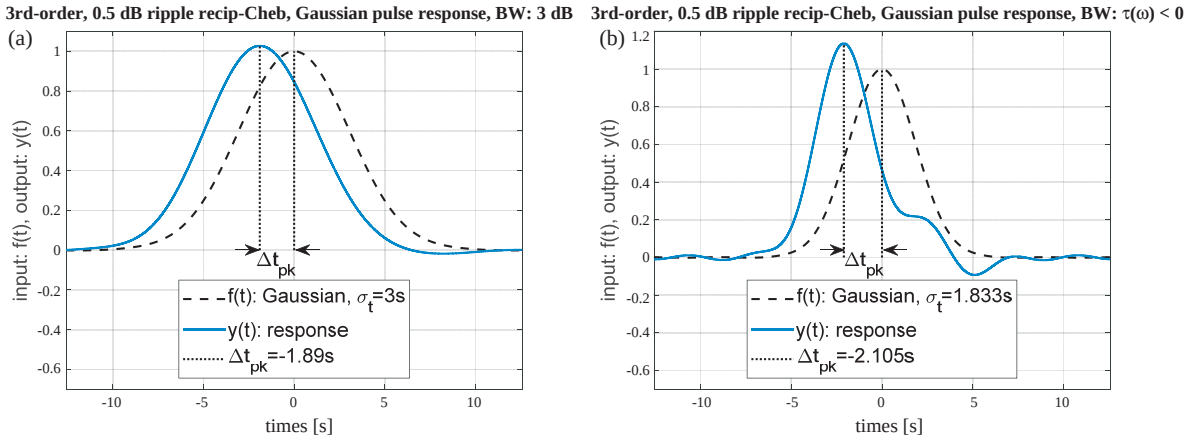

FIGURE 15. Capped reciprocal-Chebyshev 3rd-order gain-compensated design response to an input Gaussian pulse with its frequency spectrum (a) within the 3 dB-bandwidth of the design, and (b) within the $\tau(\omega) < 0$ bandwidth (1.637x wider bandwidth, leading to a distortion metric 4.26x higher than that of a 1st-order low-pass filter reference).

TABLE 1. NGD performance metrics for selected Nth-order capped reciprocal-Chebyshev baseband designs, with 3 dB-bandwidth.

Design order/ in-band ripple	Out-of-band gain, A [dB]	NGD-BW product, $-\tau(0) \cdot \Delta f_{3\,\mathrm{dB}}$	FOM [1/dB]	$\Delta t_{pk} \cdot \Delta f_{3\,\mathrm{dB}}$ (Gaussian)	Distortion: $D_{\text{in-band}}$ (Gaussian)
3rd-order Butterworth	40	0.4995	0.0125	0.5416	0.0227 ($0.55 \times D_{\text{1st-LP-filter}}$)
3rd-order, 0.25 dB	40	0.5790	0.0145	0.5904	0.0219 ($0.53 \times D_{\text{1st-LP-filter}}$)
3rd-order, 0.5 dB	40	0.6192	0.0155	0.6016	0.0260 ($0.63 \times D_{\text{1st-LP-filter}}$)
5th-order, 0.25 dB	40	0.7638	0.0191	0.7800	0.0353 ($0.86 \times D_{\text{1st-LP-filter}}$)
5th-order, 0.5 dB	40	0.8226	0.0206	0.7920	0.0413 ($1.01 \times D_{\text{1st-LP-filter}}$)
7th-order, 0.25 dB	40	0.8660	0.0217	0.8840	0.0472 ($1.15 \times D_{\text{1st-LP-filter}}$)
7th-order, 0.5 dB	40	0.9404	0.0235	0.8928	0.0541 ($1.32 \times D_{\text{1st-LP-filter}}$)

TABLE 2. NGD performance metrics for selected Nth-order capped reciprocal-Chebyshev baseband designs, with $\tau(\omega) < 0$ bandwidth.

Design order/ in-band ripple	Out-of-band gain, A [dB]	NGD-BW product, $-\tau(0) \cdot \Delta f_{\tau<0}$	$BW_{\tau<0}/BW_{3\,\mathrm{dB}}$	$\Delta t_{pk} \cdot \Delta f_{\tau<0}$ (Gaussian)	Distortion: $D_{\text{in-band}}$ (Gaussian)
3rd-order Butterworth	40	1.0761	2.154	1.1592	0.3008 ($7.32 \times D_{\text{1st-LP-filter}}$)
3rd-order, 0.25 dB	40	0.9959	1.720	1.1176	0.1958 ($4.76 \times D_{\text{1st-LP-filter}}$)
3rd-order, 0.5 dB	40	1.0137	1.637	1.0968	0.1749 ($4.26 \times D_{\text{1st-LP-filter}}$)
5th-order, 0.25 dB	40	0.9433	1.235	1.0752	0.1203 ($2.93 \times D_{\text{1st-LP-filter}}$)
5th-order, 0.5 dB	40	0.9896	1.203	1.0496	0.1121 ($2.73 \times D_{\text{1st-LP-filter}}$)
7th-order, 0.25 dB	40	0.9656	1.115	1.0456	0.0942 ($2.29 \times D_{\text{1st-LP-filter}}$)
7th-order, 0.5 dB	40	1.0325	1.098	1.0288	0.0905 ($2.20 \times D_{\text{1st-LP-filter}}$)

In comparison, the corresponding 5th-order capped reciprocal-Butterworth design yields a higher $\tau(\omega) < 0$ to 3 dB-bandwidth ratio of 1.585 (compared to 1.203) and a higher distortion metric of 0.1842 (compared to 0.1121).

As another example, a 3rd-order capped reciprocal-Chebyshev design example, with a 40 dB out-of-band gain and a 0.5 dB in-band ripple magnitude, yields to 3 dB-bandwidth and $\tau(\omega) < 0$ bandwidth responses shown in Figs. 15(a) and 15(b), respectively. The $\tau(\omega) < 0$ bandwidth response leads to an unacceptable level of pulse distortion (4.26 times higher than distortion metric of a 1st-order low-pass filter, used as reference), as demonstrated in Fig. 15(b).

10. CONCLUSION

In this paper, a prototype baseband NGD filter is introduced, based on the ratio of two transfer functions of a classical Chebyshev low-pass filter (capped reciprocal-Chebyshev design). The baseband design can be translated to a higher center frequency, yielding an NGD band-stop filter (BSF) with finite attenuation. It was shown that resonator-based design implementations in a Sallen-Key topology, as well as in an all-passive ladder topology, are feasible for the prototype NGD transfer function translated to a higher center frequency.

The prototype capped reciprocal-Chebyshev design achieves an NGD-bandwidth product that in the upper asymptotic limit for high design odd-order values is the same linear function of out-of-band gain in decibels associated with capped reciprocal-Butterworth design in [13], but further improved by an offset which is approximately a linear function of the design order. Parameters of this offset function are shown to be proportional to the in-band ripple value.

An in-band combined magnitude/phase distortion metric discussed in [13] was calculated for a Gaussian pulse input applied to several capped reciprocal-Chebyshev designs. It was shown that if the distortion metric for the proposed design and the applied waveform is to be kept below the corresponding reference distortion value of a 1st-order low-pass filter, the reduction of the in-band ripple is more effective than bandwidth reduction (which was effective for capped reciprocal-Butterworth designs [13]). Table 1 shows a performance comparison of selected proposed capped reciprocal-Chebyshev designs with a given order. The table shows achieved NGD in both the frequency and time (for a Gaussian pulse input) domains. The associated Figure-of-Merit (FOM) and distortion metric are also shown, along with the metrics for a capped reciprocal-Butterworth design from [13], for comparison. For a prescribed distortion metric value, for the same design order and out-of-band gain, it is demonstrated that the proposed capped reciprocal-Chebyshev design can achieve a higher NGD-bandwidth product than the capped reciprocal-Butterworth design reported in [13].

Further, it was shown that the bandwidth over which the group delay response is negative, $\tau(\omega) < 0$ is larger than the 3 dB-bandwidth for the presented reciprocal-capped Chebyshev design, just like it was for the capped reciprocal-Butterworth design in [13]. As a result, magnitude response variation over the $\tau(\omega) < 0$ bandwidth is higher than 3 dB and can result in an unacceptably high distortion. Table 2 summarizes NGD performance metrics for the same examples from Table 1, when instead of the 3 dB-bandwidth, the larger $\tau(\omega) < 0$ bandwidth is used. As discussed in this paper, as well as in [10, 13], any NGD design and its specified bandwidth should be checked for distortion with waveforms corresponding to that bandwidth.

REFERENCES

[1] Brillouin, L., *Wave Propagation and Group Velocity*, Academic Press, New York, 2013.

[2] Mojahedi, M., K. J. Malloy, G. V. Eleftheriades, J. Woodley, and R. Y. Chiao, "Abnormal wave propagation in passive media," *IEEE Journal of Selected Topics in Quantum Electronics*, Vol. 9, No. 1, 30–39, 2003.

[3] Stenner, M. D., D. J. Gauthier, and M. A. Neifeld, "Fast causal information transmission in a medium with a slow group velocity," *Physical Review Letters*, Vol. 94, No. 5, 053902, 2005.

[4] Wang, Y., Y. Zhang, L. He, F. Liu, H. Li, and H. Chen, "Direct observation of negative phase velocity and positive group velocity in time domain for composite right/left-handed transmission lines," *Journal of Applied Physics*, Vol. 100, No. 11, 113503, 2006.

[5] Mojahedi, M., E. Schamiloglu, F. Hegeler, and K. J. Malloy, "Time-domain detection of superluminal group velocity for single microwave pulses," *Physical Review E*, Vol. 62, No. 4, 5758, 2000.

[6] Ibraheem, I. A., J. Schoebel, and M. Koch, "Group delay characteristics in coplanar waveguide left-handed media," *Journal of Applied Physics*, Vol. 103, No. 2, 024903, 2008.

[7] Bolda, E. L., R. Y. Chiao, and J. C. Garrison, "Two theorems for the group velocity in dispersive media," *Physical Review A*, Vol. 48, No. 5, 3890, Nov. 1993.

[8] Kandic, M. and G. E. Bridges, "Asymptotic limits of negative group delay in active resonator-based distributed circuits," *IEEE Transactions on Circuits and Systems I: Regular Papers*, Vol. 58, No. 8, 1727–1735, Aug. 2011.

[9] Kandic, M. and G. E. Bridges, "Limits of negative group delay phenomenon in linear causal media," *Progress In Electromagnetics Research*, Vol. 134, 227–246, 2013.

[10] Kandic, M. and G. E. Bridges, "Negative group delay prototype filter based on cascaded second order stages implemented with sallen-key topology," *Progress In Electromagnetics Research B*, Vol. 94, 1–18, 2021.

[11] Solli, D., R. Y. Chiao, and J. M. Hickmann, "Superluminal effects and negative group delays in electronics, and their applications," *Physical Review E*, Vol. 66, No. 5, 056601, 2002.

[12] Dorrah, A. H. and M. Mojahedi, "Nonanalytic pulse discontinuities as carriers of information," *Physical Review A*, Vol. 93, No. 1, 013823, 2016.

[13] Kandic, M. and G. E. Bridges, "Negative group delay prototype filter based on the reciprocal transfer function of a low-pass Butterworth filter capped at finite out-of-band gain," *Progress In Electromagnetics Research B*, Vol. 106, 17–38, 2024.

[14] Macke, B., B. Ségard, and F. Wielonsky, "Optimal superluminal systems," *Physical Review E*, Vol. 72, No. 3, 035601, Sep. 2005.

[15] Macke, B. and B. Ségard, "Propagation of light-pulses at a negative group-velocity," *The European Physical Journal D — Atomic, Molecular, Optical and Plasma Physics*, Vol. 23, 125–141, 2003.

[16] Lucyszyn, S., I. D. Robertson, and A. H. Aghvami, "Negative group delay synthesiser," *Electronics Letters*, Vol. 29, No. 9, 798–800, Apr. 1993.

[17] Nakanishi, T., K. Sugiyama, and M. Kitano, "Demonstration of negative group delays in a simple electronic circuit," *American Journal of Physics*, Vol. 70, No. 11, 1117–1121, Nov. 2002.

[18] Kitano, M., T. Nakanishi, and K. Sugiyama, "Negative group delay and superluminal propagation: An electronic circuit approach," *IEEE Journal of Selected Topics in Quantum Electronics*, Vol. 9, No. 1, 43–51, Jan.–Feb. 2003.

[19] Siddiqui, O. F., M. Mojahedi, and G. V. Eleftheriades, "Periodically loaded transmission line with effective negative refractive index and negative group velocity," *IEEE Transactions on Antennas and Propagation*, Vol. 51, No. 10, 2619–2625, Oct. 2003.

[20] Ravelo, B., A. PÉrennec, M. L. Roy, and Y. G. Boucher, "Active microwave circuit with negative group delay," *IEEE Microwave*

and Wireless Components Letters, Vol. 17, No. 12, 861–863, Dec. 2007.

[21] Mirzaei, H. and G. V. Eleftheriades, "Realizing non-Foster reactive elements using negative-group-delay networks," *IEEE Transactions on Microwave Theory and Techniques*, Vol. 61, No. 12, 4322–4332, Dec. 2013.

[22] Chaudhary, G., Y. Jeong, and J. Lim, "Microstrip line negative group delay filters for microwave circuits," *IEEE Transactions on Microwave Theory and Techniques*, Vol. 62, No. 2, 234–243, Feb. 2014.

[23] Wu, C.-T. M. and T. Itoh, "Maximally flat negative group-delay circuit: A microwave transversal filter approach," *IEEE Transactions on Microwave Theory and Techniques*, Vol. 62, No. 6, 1330–1342, Jun. 2014.

[24] Wu, Y., H. Wang, Z. Zhuang, Y. Liu, Q. Xue, and A. A. Kishk, "A novel arbitrary terminated unequal coupler with bandwidth-enhanced positive and negative group delay characteristics," *IEEE Transactions on Microwave Theory and Techniques*, Vol. 66, No. 5, 2170–2184, 2018.

[25] Wan, F., N. Li, B. Ravelo, and J. Ge, "O=O shape low-loss negative group delay microstrip circuit," *IEEE Transactions on Circuits and Systems II: Express Briefs*, Vol. 67, No. 10, 1795–1799, Oct. 2020.

[26] Ravelo, B., F. Wan, and J. Ge, "Anticipating actuator arbitrary action with a low-pass negative group delay function," *IEEE Transactions on Industrial Electronics*, Vol. 68, No. 1, 694–702, Jan. 2021.

[27] Wang, Z., S. Zhao, H. Liu, and S. Fang, "A compact dual-band differential negative group delay circuit with wideband common mode suppression," *IEEE Journal of Microwaves*, Vol. 2, No. 4, 720–725, Oct. 2022.

[28] Nair, R. G. and S. Natarajamani, "Design theory of compact power divider with reconfigurable power division and negative group delay characteristics," *Scientific Reports*, Vol. 13, No. 1, 7222, May 2023.

[29] Palson, C. L., D. D. Krishna, and B. R. Jose, "Planar tunable negative group delay circuit with low reflection loss," *Progress In Electromagnetics Research Letters*, Vol. 113, 53–59, 2023.

[30] Ravelo, B., H. Bilal, S. Rakotonandrasana, M. Guerin, F. Haddad, S. Ngoho, and W. Rahajandraibe, "Transient characterization of new low-pass negative group delay RC-network," *IEEE Transactions on Circuits and Systems II: Express Briefs*, Vol. 71, No. 1, 126–130, Jan. 2024.

[31] Zhang, A., J. Xu, and Z. Liu, "A microstrip linear-phase BPF using dual-band negative group delay equalizers," *IEEE Microwave and Wireless Technology Letters*, Vol. 34, No. 4, 387–390, Apr. 2024.

[32] Chang, N., A. Yuan, Y. Wang, and J. Liu, "Multi-band pass negative group delay circuit with low insertion loss," *International Journal of Circuit Theory and Applications*, 2024.

[33] Nako, J., C. Psychalinos, A. S. Elwakil, and B. J. Maundy, "A note on the bandwidth of negative group delay filters," *International Journal of Circuit Theory and Applications*, 2024.

[34] Nako, J., C. Psychalinos, B. J. Maundy, and A. S. Elwakil, "Elementary negative group delay filter functions," *Circuits, Systems, and Signal Processing*, Vol. 43, No. 6, 3396–3409, 2024.

[35] Maundy, B. J., A. S. Elwakil, and C. Psychalinos, "Systematic design of negative group delay circuits," *AEU — International Journal of Electronics and Communications*, Vol. 174, 155060, 2024.

[36] Nako, J., C. Psychalinos, A. S. Elwakil, and B. J. Maundy, "Power-law negative group delay filters," *Electronics*, Vol. 13, No. 3, 522, 2024.

[37] United States Patent Office (USPTO) application number: 18/491922.